Article

Discovery Medicine 2026; 38(212): 2800–2812
https://doi.org/10.24976/Discov.Med.202638212.216

Astragaloside IV Alleviates Transferrin Receptor 1-Mediated Ferroptosis in Diabetic Nephropathy

Fei Zhou[1], Jialei Zhou[2,*]

[1]Department of Endocrinology, The First People's Hospital of Xiaoshan District, 311200 Hangzhou, Zhejiang, China
[2]Department of Clinical Laboratory, The First People's Hospital of Xiaoshan District, 311200 Hangzhou, Zhejiang, China
*Correspondence: zhoujialei89@163.com (Jialei Zhou)
Submitted: 22 May 2026 Revised: 18 June 2026 Accepted: 6 July 2026 Published: 23 September 2026

Background: Diabetic nephropathy (DN) is a leading cause of end-stage renal disease with limited therapeutic options. Astragaloside IV (AS-IV), a saponin monomer from Radix Astragali, has been reported to exert renoprotective effects; however, the underlying mechanism remains unclear. Network pharmacology identified transferrin receptor 1 (TFRC) as a potential target of AS-IV. This study investigated whether AS-IV alleviates DN by modulating TFRC-mediated ferroptosis.

Methods: A DN rat model was established via intraperitoneal injection of streptozotocin (STZ). Successfully modelled rats were randomized into three groups (n = 6 each): DN model, Ferrostatin-1 (ferroptosis inhibitor, positive control), and AS-IV (5 mg/kg/d, oral administration). A negative control group received saline. Treatments were initiated 3 weeks after STZ injection and continued for 12 weeks. To evaluate the renoprotective effects of AS-IV, we measured fasting blood glucose, renal function (serum creatinine (Scr), blood urea nitrogen (BUN), urinary albumin excretion rates (UAER)), and performed histopathological (Hematoxylin-Eosin (HE)/Masson) and TUNEL staining. To dissect the molecular mechanism, we examined ferroptosis markers (glutathione peroxidase 4 (*GPX4*), solute carrier family 7 member 11 (*SLC7A11*), ferritin heavy chain 1 (*FTH-1*)) by qRT-PCR, lipid peroxidation indices (malondialdehyde (MDA), 4-Hydroxynonenal (4-HNE), glutathione (GSH), iron content), and the TFRC/nuclear factor erythroid 2-related factor 2 (Nrf2)/heme oxygenase-1 (HO-1) protein axis by Western blotting. For *in vitro* validation, HK-2 cells were exposed to high glucose, treated with AS-IV with or without TFRC overexpression, and assessed for cell viability, apoptosis, lipid peroxidation, and pathway protein expression.

Results: AS-IV treatment significantly improved renal function, ameliorated renal histopathological lesions, and reduced tubular and glomerular injury scores in DN rats ($p < 0.05$). It also attenuated renal cell apoptosis ($p < 0.001$). Mechanistically, AS-IV downregulated TFRC protein expression, activated the Nrf2/HO-1 signalling axis, restored the mRNA expression of the ferroptosis-related markers GPX4, SLC7A11 and FTH-1, reduced lipid peroxidation products and iron content, and increased GSH levels ($p < 0.01$). In high glucose-treated HK-2 cells, AS-IV enhanced cell viability and reduced apoptosis, lactate dehydrogenase release, reactive oxygen species, Fe^{2+} and MDA; however, these protective effects were partially reversed by TFRC overexpression ($p < 0.01$).

Conclusion: AS-IV alleviates renal injury and ferroptosis in DN, and this effect is associated with downregulation of TFRC and activation of the Nrf2/HO-1 pathway. These findings suggest that TFRC may be involved in the protective effects of AS-IV and warrants further investigation as a potential therapeutic target.

Keywords: DN; AS-IV; TFRC; Nrf2/HO-1 axis

Introduction

Diabetic Nephropathy (DN) is a microvascular complication characterised by proteinuria and progressive loss of renal function [1,2]. The pathological features of DN primarily include glomerular basement membrane thickening, extracellular matrix deposition, interstitial fibrosis, nodular glomerulosclerosis formation, and reduced endothelial cell counts. Its clinical features are manifested by persistent albuminuria and/or progressive decrease in glomerular filtration rate. DN is not only one of the most serious microvascular complications of diabetes mellitus, but also a major cause of end-stage renal disease [3]. It is estimated that 30% of patients with type 1 diabetes and 40% of patients with type 2 diabetes will progress to DN [4], posing a severe economic and social burden on the national healthcare system. Currently, basic clinical treatments for DN include control of blood glucose and blood pressure, and inhibition of the renin-angiotensin system [5,6]. Additionally, newer therapeutic agents such as glucagon-like peptide-1 (GLP-1) receptor agonists, sodium-glucose cotransporter 2 (SGLT2) inhibitors, and the nonsteroidal mineralocorticoid receptor antagonist finerenone have shown significant renoprotective benefits in clinical trials. However, despite these advances, DN often progresses to end-stage renal disease, underscoring the need for further research into its pathogenesis and the development of novel treatments.

Traditional Chinese Medicine (TCM) has been increasingly investigated for its therapeutic potential in DN, with accumulating evidence suggesting that herbal formulas and active compounds can ameliorate renal injury through multi-target regulatory mechanisms [7,8,9]. *Radix Astragali*, a leguminous plant in the family of legumes [10], is one of the TCMs that the project team has investigated for a long time. The root of *Radix Astragali* is regarded as the 'king of TCM' because of its rich medicinal value. Astragaloside IV (AS-IV), a saponin monomer compound, is one of the signature active ingredients of *Radix Astragali* [11]. AS-IV exhibits a range of pharmacological activities, including improving endothelial cell and neovascular function, as well as exerting anti-inflammatory, antioxidant, neuroprotective, anticancer and other effects [11,12,13]. In addition, it has a preventive effect on organic lesions of many organs, including the kidney [14]. Using the BATMAN-TCM database (http://bionet.ncpsb.org/batman-tcm/) to predict targets for AS-IV, we identified the ferroptosis key gene transferrin receptor 1 (TFRC) as a potential target for AS-IV. Ferroptosis is a novel form of Fe-dependent regulated cell death characterised by changes in iron overload, loss of antioxidant capacity and the peroxidation of phospholipid-bound polyunsaturated fatty acids [15]. Recent studies have shown that ferroptosis is observed in a variety of renal diseases, including acute kidney injury, renal ischaemia-reperfusion injury and DN [15,16,17,18]. Key markers of ferroptosis include dysregulation of proteins such as glutathione peroxidase 4 (GPX4), solute carrier family 7 member 11 (SLC7A11), and ferritin heavy chain 1 (FTH-1), along with increased levels of lipid peroxidation products (e.g., malondialdehyde (MDA), 4-Hydroxynonenal (4-HNE)) and depletion of antioxidants like glutathione (GSH) [19,20,21]. Measurement of these biomarkers provides a direct assessment of ferroptosis activity.

This study aimed to investigate the mechanism by which AS-IV modulates TFRC to affect ferroptosis in DN. We employed a streptozotocin-induced DN rat model and a high glucose (HG)-induced HK-2 cell model to assess changes in metabolic parameters, renal function and histology, ferroptosis-related markers, and the TFRC/nuclear factor erythroid 2-related factor 2 (Nrf2)/heme oxygenase-1 (HO-1) signaling pathway.

Materials and Methods

Animals

We purchased 27 Sprague-Dawley (SD) rats (males, 100 ±10 g) from Hangzhou Medical College. All rats were housed in a specific pathogen free (SPF)-grade animal centre, which provided rats with free access to water and diet. All animal experiments were approved by the Institutional Animal Care and Use Committee of Zhejiang Center of Laboratory Animals (Approval Number: ZJCLA-IACUC-20030149), and the experimental procedures followed the relevant regulations for the ethical protection of animals and the ARRIVE Guidelines 2.0, with every effort made to minimise animal suffering.

Construction of Animal Models and Group Treatment

After 3 days of acclimatisation, rats were randomly divided into two groups synchronously using a random number table: a negative control (NC) group (n = 6) and a DN model group (n = 21). The DN rat model was induced using the classical streptozotocin (STZ; CAS No.: 18883-66-4, Item No.: S17049, Shanghai yuanye Bio-Technology Co., Ltd., Shanghai, China) induction method [22]. After 12 hours of fasting without water, 65 mg/kg of STZ was injected into rats via the intraperitoneal cavity. Rats in the NC group were injected with an equal volume of saline. The success of the model construction was determined by the blood glucose level of the rats after 48 h (rats with blood glucose >300 mg/dL). 18 DN rats were obtained, whereas 3 rats that failed to meet the predefined blood glucose criterion were euthanised. Thereafter, blood glucose was continuously monitored after STZ induction. Before initiating drug treatment, we collected 24 h urine and blood samples from model rats and measured urinary albumin (uALB), blood urea nitrogen (BUN) and serum creatinine (Scr) to confirm the establishment of DN. 18 DN model rats were randomly divided into 3 groups (n = 6/group): the DN model (DM) group, the Ferrostatin-1 (Fer-1) treatment group, and the AS-IV treatment group. After 3 weeks of STZ injection, rats in the AS-IV group were orally administered 5 mg/kg of AS-IV (Catalogue No.: HY-N0431, MedChemExpress, Monmouth Junction, NJ, USA) daily [22]; whereas rats in the Fer-1 group were intraperitoneally injected with 5 mg/kg of Fer-1 (Catalogue No.: HY-100579, MedChemExpress, USA; Solvent: 5% DMSO + 95% corn oil) daily [23], these treatments lasted for 12 weeks. The initiation of STZ injection was defined as week 0, we measured the body weight of rats in each group at 0 week (w), 3 w, 6 w, 9 w, 12 w and 15 w of the experiment. At the endpoint of the 15-w experiment period, all rats were euthanised by intraperitoneal injection of an overdose of sodium pentobarbital (150 mg/kg).

Fasting Blood Glucose and Renal Function Tests

After 12 hours of dietary abstinence, blood was collected from the tail vein of rats, and fasting blood glucose was measured using a glucose meter. The collected blood was centrifuged to separate the serum, and then a rat Scr kit (Item No. C011-2-1, Nanjing Jiancheng Bioengineering Institute, Nanjing, China) and rat BUN kit (Item No.: C013-2-1, Nanjing Jiancheng Bioengineering Institute, Nanjing, China) were used for the detection of Scr and BUN. 24-hour urine collected from rats was centrifuged for 20 minutes to obtain the supernatant, and the supernatant was analyzed with a rat uALB ELISA kit (Item No.: ml106998, mlbio,

Shanghai, China). Urinary albumin excretion rates (UAER, mg/24 h) = uALB concentration (mg/L) × 24 h urine volume (L).

Pathological Staining and Scoring

The right kidney of rats (n = 3/group) was immersed and fixed in 4% paraformaldehyde for 24 hours. After gradient dehydration treatment, the kidney tissues were embedded in paraffin and cut into 4-μm sections. After dewaxing and hydration, kidney sections were treated with hematoxylin and eosin stains in turn according to the operating instructions of the Hematoxylin-Eosin (HE) Stain Kit (Cat: G1120, Solarbio, Beijing, China). In addition to HE staining, the Masson's Trichrome Stain Kit (Cat: G1340, Solarbio, China) was used to stain the kidney sections. After sealing, the sections were observed under a microscope (Cat: DX51, OLYMPUS, Tokyo, Japan) at a magnification of 400 times.

After obtaining 50 randomly selected glomerular images per animal, glomerular damage scores were assigned based on the percentage of glomerular involvement (with mesangial expansion and matrix deposition) using the following grading system [24]: 0 points indicate normal; 1 point refers to less than 25% glomerular involvement; 2 points refer to 25%–50% glomerular involvement; 3 points refer to 50%–75% glomerular involvement; 4 points refer to 75%–100% glomerular involvement. Tubulointerstitial injury was evaluated based on histopathological changes, such as tubulointerstitial fibrosis, tubular necrosis, tubular epithelial desquamation, and tubular oedema. Therefore, 20 randomly selected areas in the renal cortex were examined and the extent of tubulointerstitial injury was quantified (including interstitial fibrosis, tubular atrophy, tubular dilatation, and cast formation) [24]: grade 0 indicates no injury; grade 1 indicates impairment <10%; grade 2 indicates impairment 10–25%; grade 3 indicates impairment 26–50%; grade 4 indicates impairment 51–75%; grade 5 indicates impairment >75%.

TUNEL Staining

Apoptosis was detected using a One-step TUNEL *In Situ* Apoptosis Kit (Item No. E-CK-A320, Elabscience®, Wuhan, China) according to the manufacturer's protocol. The right kidney of rats (n = 3/group) was sectioned into frozen slices. After equilibration to room temperature, the sections were fixed in 4% paraformaldehyde for 30 minutes. For *in vitro* studies, cell crawls were fixed in 4% paraformaldehyde for 1 hour. After the sections or cell coverslips were fixed, they were permeabilized with 0.1% Triton X-100 for 8 min at room temperature, and incubated with Equilibration Buffer. The samples were then incubated with the TUNEL reaction mixture containing TdT enzyme and fluorescently labeled dUTP at 37 °C for 60 min in the dark, followed by counterstaining with DAPI for nuclear visualization. After sealing, the sections were observed under a fluorescence microscope (model: Eclipse E800, Nikon, Japan) to evaluate the staining results.

Cell Culture and Processing

Human renal cortical proximal tubule epithelial cells HK-2 (Item No.: CL-0109, Wuhan Pricella Biotechnology Co., Ltd., Wuhan, China) were cultured in growth medium (MEM medium + 10% fetal bovine serum + 1% penicillin-streptomycin). The medium (Item No.: PM150410), fetal bovine serum (Item No.: 164210-50), and penicillin-streptomycin (Item No.: PB180120) were provided by Wuhan Pricella Biotechnology Co. HK-2 cells were authenticated by STR profiling and tested to be free of mycoplasma contamination.

The cell model was established using classical HG treatment by adding 30 mM D-glucose to the culture medium of HK-2 cells and cultured for 48 h [25]. Normal HK-2 cells (labelled as NG group) were then exposed to 5.5 mM D-glucose. In the *in vitro* study, AS-IV was treated at a concentration of 100 μg/mL for 24 h [22]. For TFRC overexpression, the human TFRC coding sequence (NM_001128148.3) was inserted into the pc-DNA3.1 vector (V79020, Thermo Fisher Scientific, Waltham, MA, USA) to obtain a TFRC overexpression plasmid. An empty pc-DNA3.1 vector was used as the negative control (NC). Subsequently, the above plasmids were transfected into HK-2 cells using Lipofectamine™ 3000 (Item no.: L3000015, Thermo Fisher Scientific, Waltham, MA, USA). 48 h later, the plasmids were detected using quantitative real-time polymerase chain reaction (qRT-PCR) to assess the transfection efficiency.

Western Blotting

Rat kidney tissues were homogenized into a slurry. RIPA buffer (Cat No.: R0010, Solarbio, China) was added to extract total proteins from kidney tissues or HK-2 cells. Protein concentration was determined by the classical BCA method with the Pierce™ BCA Protein Assay Kits (Cat No.: 23225, Thermo Scientific, Waltham, MA, USA). Protein samples after high-temperature denaturation were injected into SDS-PAGE gels. The separated proteins were transferred onto PVDF membrane (Item No.: ISEQ00010, Millipore, Burlington, MA, USA). After the transfer, the PVDF membrane was incubated sequentially with diluted primary and secondary antibodies. The dilution ratios of the antibodies and the information on their use are listed in Table 1. The protein bands were analysed using Tanon gel imager (Tanon-5200, TANON, Shanghai, China) and ImageJ software (version 1.52s, National Institutes of Health, Bethesda, MA, USA). β-actin served as the loading control. Relative protein level = target protein / β-actin (internal reference).

Table 1. Antibodies used in Western blotting.

Antibodies	Dilution rate	Molecular weight	Production No.
TFRC	1/1000	90 kDa	ab214039, Abcam, UK
Nrf2	1/1000	110 kDa	ab325240, Abcam, UK
HO-1	1/2000	33 kDa	ab189491, Abcam, UK
β-actin	1/5000	42 kDa	ab6276, Abcam, UK
Goat Anti-Rabbit IgG H&L	1/5000	—	ab6721, Abcam, UK
Goat Anti-Mouse IgG H&L	1/5000	—	ab150113, Abcam, UK

TFRC, transferrin receptor 1; Nrf2, nuclear factor erythroid 2-related factor 2; HO-1, heme oxygenase-1.

Table 2. Primers for qRT-PCR.

Gene name	Species	Forward primer (5′→3′)	Reverse primer (5′→3′)
GPX4	Rat	GAGGCAAGACCGAAGTAAACTAC	CCGAACTGGTTACACGGGAA
SLC7A11	Rat	AACTGCTGGTAATACGCCCC	GGAAAATCTGGATCCGGGCA
FTH-1	Rat	AGCTCTACGCCTCCTACGTT	AAGGAAGATTCGGCCACCTC
TFRC	Rat	CCTATATGCTTGGGTAGGAGGC	TACAAGGGAGCACTCTGAAGC
	Human	ACCATTGTCATATACCCGGTTCA	CAATAGCCCAAGTAGCCAATCAT
β-actin	Rat	TGCCTGACGGTCAGGTCA	CAGGAAGGAAGGCTGGAAG
	Human	CAAATGCTTCTAGGCGGACTATG	TGCGCAAGTTAGGTTTTGTCA

qRT-PCR, quantitative real-time polymerase chain reaction; *GPX4*, glutathione peroxidase 4; *SLC7A11*, solute carrier family 7 member 11; *FTH-1*, ferritin heavy chain 1.

qRT-PCR

To obtain RNA from kidney tissues or HK-2 cells, TRIzol reagent (Item No.: 15596026, Invitrogen, Carlsbad, CA, USA) was added, and total RNA was isolated by centrifugation. Extracted RNA was converted into cDNA following the instructions of the SuperScript™ VILO™ cDNA Synthesis Kit (Item No.: 11754250, Invitrogen, Carlsbad, CA, USA). Primers targeting the genes of interest (Table 2) were synthesised by Sangon Biotech (shanghai, China). qPCR assay was performed using the Fast7500 Real-Time Fluorescence Quantitative PCR System (Item No.: 4351107, Applied Biosystems, Foster City, CA, USA). Relative mRNA levels were calculated using the $2^{-\Delta\Delta CT}$ formula. *β-actin* served as the loading control.

Detection of Indicators Related to Ferroptosis

For the detection of lipid peroxidation, lactate dehydrogenase (LDH) activity, reactive oxygen species (ROS), the following kits were used: malondialdehyde (MDA; Item No.: E-BC-F007, Elabscience, Wuhan, China), 4-Hydroxynonenal (4-HNE; Item No.: ml095918, mlbio, Shanghai, China), glutathione (GSH; Item No.: E-BC-K030-M, Elabscience, China), rat serum iron content (Item No.: TW5641, TW-reagent, Shanghai, China), LDH (Item No. E-BC-K771-M, Elabscience, China), ROS (Item No. E-BC-K138-F, Elabscience, China), and Fe^{2+} level (Item No. E-BC-F101, Elabscience, China).

For serum samples, rat serum was collected and processed according to the operational requirements of each kit. For cell samples, cells were harvested, resuspended in serum-free medium, and processed according to the operational requirements of each kit. After termination of the reaction, the absorbance of each relevant indicator was measured using the SpectraMax Plus 384 microplate reader (Molecular Devices, Sunnyvale, CA, USA) or SpectraMax Gemini EM microplate reader (Molecular Devices, Sunnyvale, CA, USA). All detection wavelengths were set according to the manufacturer's instructions.

Cell Counting Kit (CCK)-8 Assay

After AS-IV and/or TFRC treatment, CCK-8 reagent (Cat. No.: HY-K0301, MedChemExpress, USA) was added to 96-well plates, and incubated with HK-2 cells (5×10^3 cells/well). After 4 hours of incubation, HK-2 cells were analysed using a microplate reader, with detection wavelength set at 450 nm.

Statistical Analysis

GraphPad Prism 8.0 software (GraphPad Software, San Diego, CA, USA) was used for statistical analysis for the entire study. Data were expressed as mean ± standard deviation (SD). The normal distribution of data was tested with the Shapiro-Wilk test. Repeated-measures two-way analysis of variance (ANOVA) or one-way ANOVA followed by Tukey's post hoc test was employed for comparisons among multiple groups. Differences were considered statistically significant at $p < 0.05$.

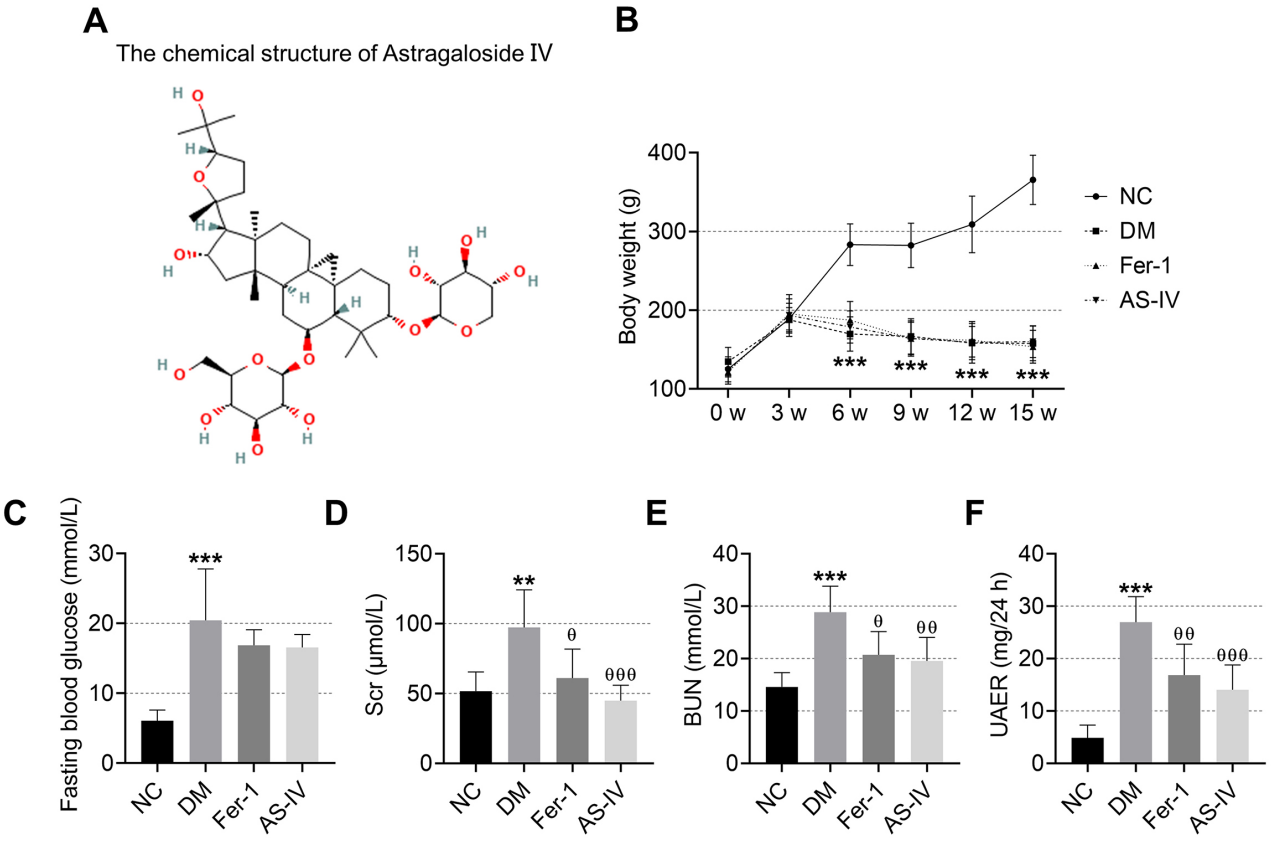

Fig. 1. AS-IV improved renal function abnormalities in DN rats. (A) Chemical structural formula of AS-IV. (B) Effects of AS-IV or Fer-1 treatment on body weight in DN rats. (C) Effects of AS-IV or Fer-1 treatment on fasting blood glucose in DN rats. (D–F) Effects of AS-IV or Fer-1 treatment on renal function in DN rats. n = 6 rats per group. Data are presented as mean ± SD from three independent experiments, each performed in triplicate. $^{**}p < 0.01$, $^{***}p < 0.001$ vs NC group; $\theta p < 0.05$, $\theta\theta p < 0.01$, $\theta\theta\theta p < 0.001$ vs DM group. Abbreviations: DN, Diabetic Nephropathy; AS-IV, Astragaloside IV; Fer-1, Ferrostatin-1; NC, negative control; DM, DN model; Scr, serum creatinine; BUN, blood urea nitrogen; UAER, urinary albumin excretion rates.

Results

AS-IV Alleviated Kidney Injury in DN Rats

Fig. 1A demonstrates the chemical structure of AS-IV. The results of the body weight test showed that compared with the NC group, the body weight of rats in the DM group was significantly reduced from the 6th week (Fig. 1B, $p < 0.001$). However, Fer-1 and AS-IV had no significant effect on the body weight of the model rats (Fig. 1B). Fasting blood glucose and renal function tests showed that rats in the DM group had significantly higher fasting blood glucose, Scr, BUN and UAER (Fig. 1C–F, $p < 0.01$). These results indicated that the model rats showed typical features of DN. After AS-IV treatment, Scr, BUN and UAER were significantly reduced in rats (Fig. 1C–F, $p < 0.01$). Fer-1, a ferroptosis inhibitor, produced similar improvement (Fig. 1C–F, $p < 0.05$). Histopathological staining showed that rats in the DM group exhibited obvious renal morphological changes and glomerular changes characterised by basement membrane dilatation (Fig. 2A). Consistently, glomerular injury score and tubulointerstitial injury score were significantly increased, indicating severe renal damage in DM rats (Fig. 2B,C, $p < 0.01$). After AS-IV and Fer-1 treatment, renal morphological changes were markedly alleviated (Fig. 2A), and both glomerular injury scores and tubulointerstitial injury scores significantly decreased (Fig. 2B,C, $p < 0.05$). TUNEL staining suggested increased apoptosis in renal cells in the DM group, while AS-IV and Fer-1 treatment significantly alleviated renal cell apoptosis (Fig. 3A,B, $p < 0.001$).

AS-IV Modulated Renal TFRC/Nrf2/HO-1 Protein Expression and Ferroptosis-Associated Markers in DN Rats

We first detected the protein expression of TFRC/Nrf2/HO-1 signaling in rat kidneys. Compared with the NC group, TFRC protein expression was significantly upregulated in the kidneys of rats in the DM group, whereas the expression of Nrf2 and HO-1 proteins was significantly suppressed (Fig. 4A–D, $p < 0.001$). However, after AS-IV or Fer-1 treatment, TFRC protein levels were downregulated, and Nrf2 and HO-1 protein expression was

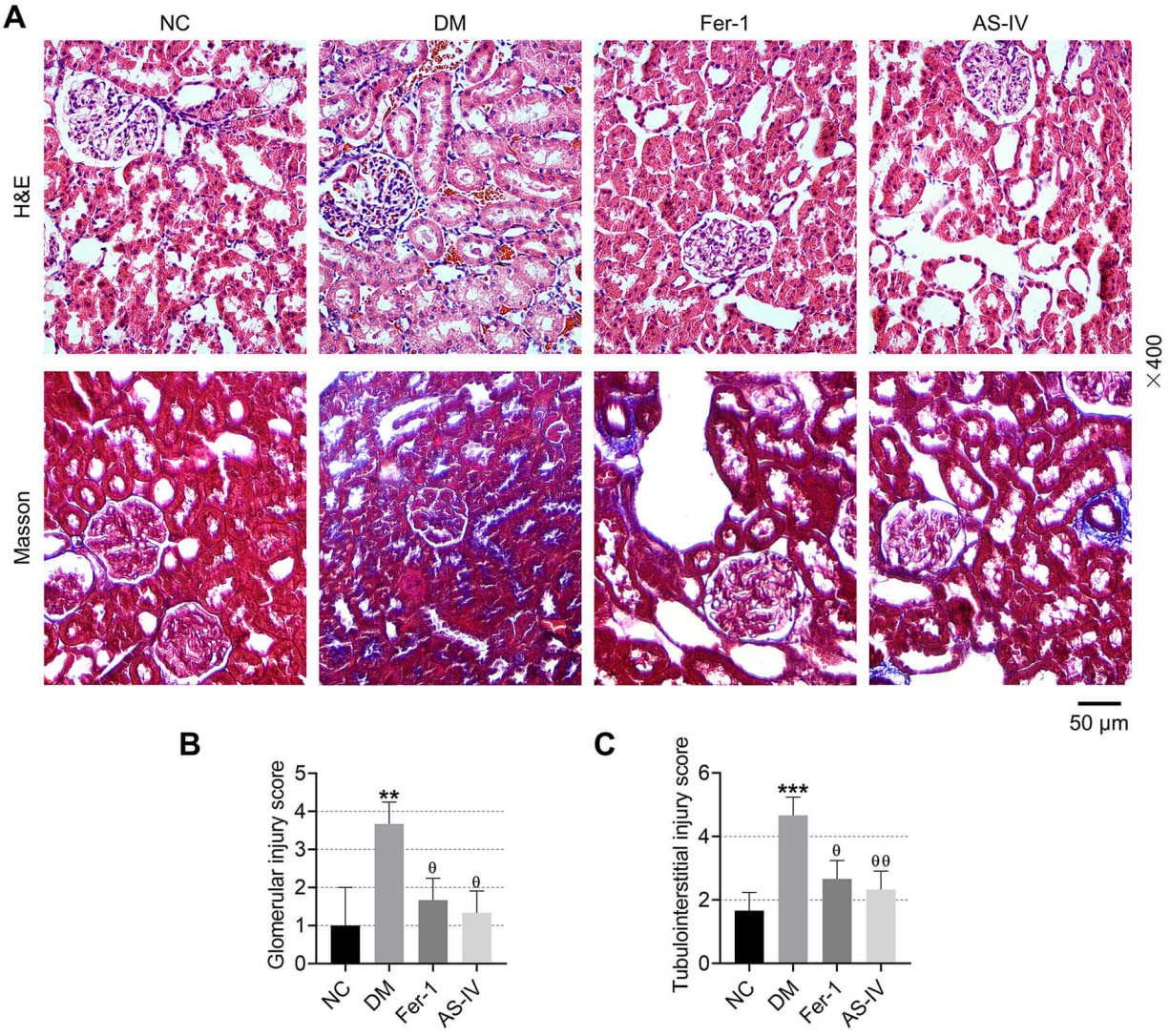

Fig. 2. AS-IV reduced kidney injury in DN rats. (A–C) The effects of AS-IV or Fer-1 treatment on the kidneys of DN rats were evaluated by Hematoxylin-Eosin and Masson staining, and the glomerular injury score and tubulointerstitial injury score were further calculated. Magnification 400×. Scale bar = 50 μm. n = 3 rats per group. Data are presented as mean ± SD from three independent experiments, each performed in triplicate. $^{**}p < 0.01$, $^{***}p < 0.001$ vs NC group; $\theta p < 0.05$, $\theta\theta p < 0.01$ vs DM group. Abbreviations: DN, Diabetic Nephropathy; AS-IV, Astragaloside IV; Fer-1, Ferrostatin-1; NC, negative control; DM, DN model.

partially restored (Fig. 4A–D, $p < 0.01$). The expression levels of *GPX4*, *SLC7A11* and *FTH-1* were decreased in the DM group compared to the NC group (Fig. 4E–G, $p < 0.001$). However, AS-IV or Fer-1 treatment upregulated the expression levels of *GPX4*, *SLC7A11* and *FTH-1*, suggesting that excessive ferroptosis in the kidney was controlled (Fig. 4E–G, $p < 0.05$). Changes in lipid peroxidation indexes also supported these findings. Compared with the NC group, the serum levels of MDA, 4-HNE and iron content were significantly increased in rats of the DM group, while GSH levels were decreased (Fig. 4H–K, $p < 0.001$). In comparison with the DM group, MDA, 4-HNE and iron content levels were decreased and GSH levels were restored in AS-IV or Fer-1 treated rats (Fig. 4H–K, $p < 0.01$).

In Vitro Experiments Demonstrated That TFRC Overexpression Partially Reversed the Effect of AS-IV on the HG-Induced Ferroptosis

Transfection efficiency experiments showed that overexpression of TFRC significantly upregulated TFRC expression in HK-2 cells (Fig. 5A, $p < 0.001$). The cell function assay showed that AS-IV alleviated HG-induced cell damage. Specifically, AS-IV up-regulated HK-2 cell viability and GSH levels, down-regulated LDH, ROS, Fe^{2+}, and MDA levels, and reduced HG-induced HK-2 cell apoptosis (Fig. 5B–I, $p < 0.01$). However, overexpression of TFRC partially counteracted the protective effect of AS-IV. As shown in Fig. 5B–I, overexpression of TFRC resulted in decreased viability and increased apoptosis in HK-2 cells, and the levels of LDH, ROS, Fe^{2+}, and MDA were up-

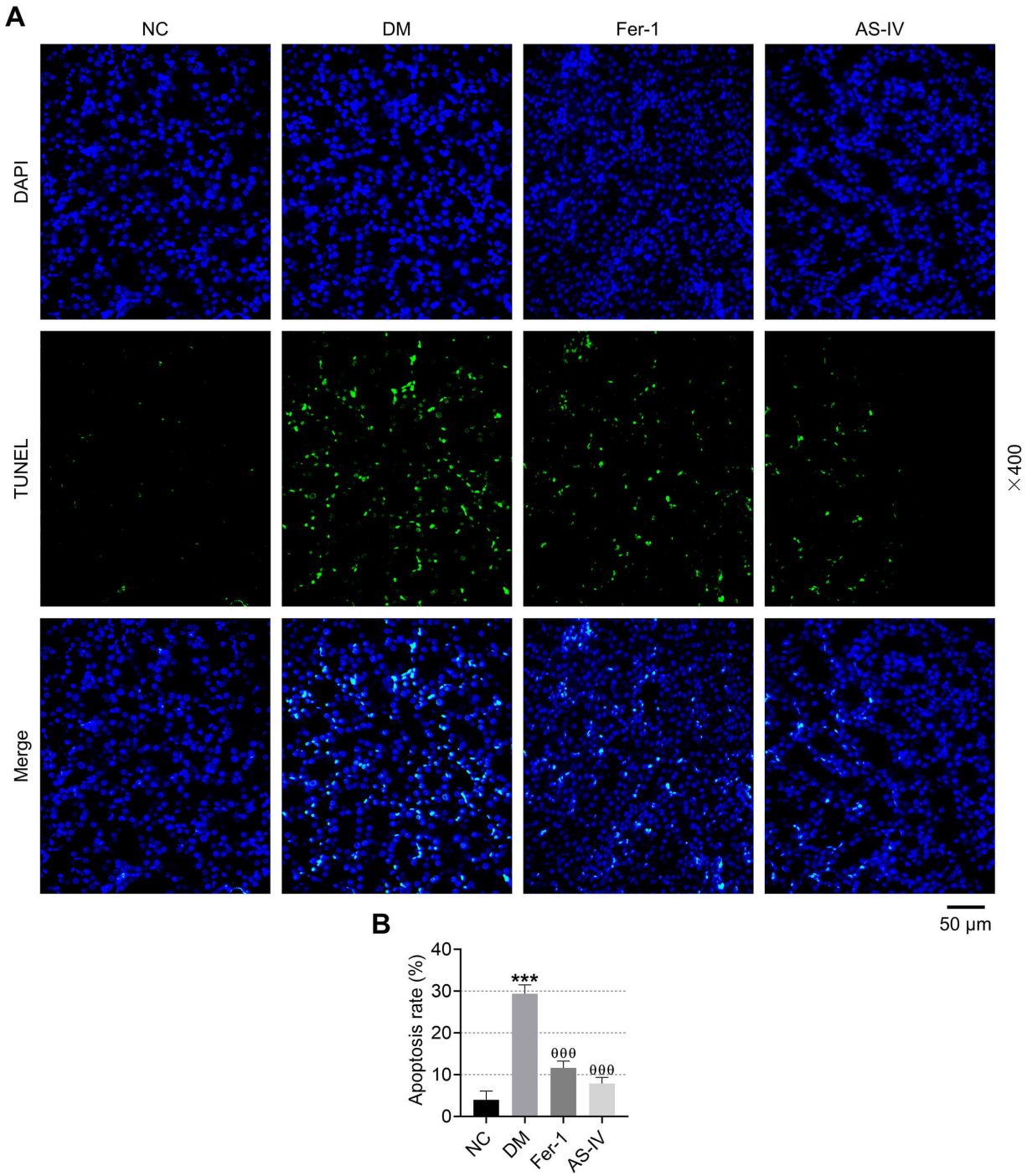

Fig. 3. AS-IV reduces apoptosis in renal cells of rats with DN. (A,B) Effects of AS-IV or Fer-1 treatment on renal cell apoptosis in DN rats were evaluated by TUNEL staining. The magnification was 400×. Scale bar = 50 μm. n = 3 rats per group. Data are presented as mean ± SD from three independent experiments, each performed in triplicate. ***$p < 0.001$ vs NC group; θθθ$p < 0.001$ vs DM group. Abbreviations: DN, Diabetic Nephropathy; AS-IV, Astragaloside IV; Fer-1, Ferrostatin-1; NC, negative control; DM, DN model.

regulated, whereas GSH levels were reduced (Fig. 5B–I, $p < 0.01$). For the TFRC/Nrf2/HO-1 axis, AS-IV treatment prevented HG-induced TFRC activation, which in turn activated the Nrf2/HO-1 axis (Fig. 6A–D, $p < 0.001$). However, TFRC overexpression treatment counteracted the regulatory effect of AS-IV (Fig. 6A–D, $p < 0.01$).

Discussion

This study demonstrates that AS-IV alleviates renal injury and dysfunction in a rat model of DN. Mechanistically, our data suggest that AS-IV downregulates TFRC to inhibit ferroptosis, accompanied by activation of the

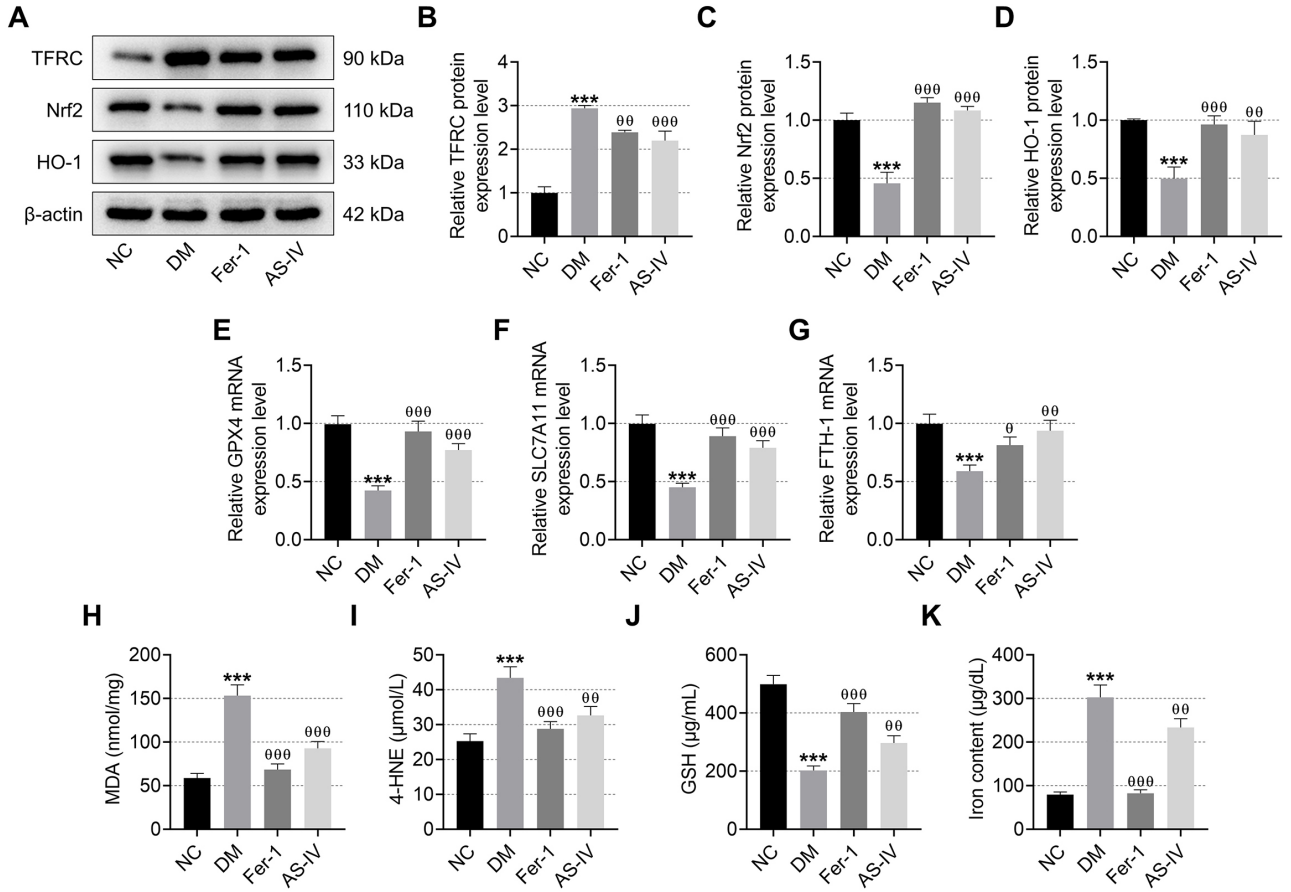

Fig. 4. AS-IV modulates renal TFRC/Nrf2/HO-1 protein expression and ferroptosis-associated markers in DN rats. (A–D) Effects of AS-IV or Fer-1 treatment on TFRC/Nrf2/HO-1 protein expression in DN rat kidneys were analysed by Western blotting. β-actin served as an internal reference protein. (E–G) Effects of AS-IV or Fer-1 treatment on the expression of ferroptosis-related indicators in DN rat kidneys were analysed by qRT-PCR. β-actin was the internal reference gene. (H–K) The effects of AS-IV or Fer-1 treatment on lipid peroxidation in DN rats were determined by the relevant indicators. n = 6 rats per group. Data are presented as mean ± SD from three independent experiments, each performed in triplicate. ***$p < 0.001$ vs NC group; θ$p < 0.05$, θθ$p < 0.01$, θθθ$p < 0.001$ vs DM group. Abbreviations: DN, Diabetic Nephropathy; AS-IV, Astragaloside IV; Fer-1, Ferrostatin-1; NC, negative control; DM, DN model; TFRC, transferrin receptor 1; *GPX4*, glutathione peroxidase 4; *SLC7A11*, solute carrier family 7 member 11; *FTH-1*, ferritin heavy chain 1; MDA, malondialdehyde; 4-HNE, 4-Hydroxynonenal; GSH, glutathione.

Nrf2/HO-1 pathway. However, it should be emphasized that these findings are primarily correlative and provide supportive evidence at the phenotypic level, rather than definitive mechanistic proof of a linear causal pathway. In recent years, ferroptosis has been increasingly recognized as a key driver in the progression of DN [15]. This is because this novel mode of cell death can interact with pathological changes such as fibrosis, inflammation, oxidative stress, and disorders of glycolipid metabolism to disrupt renal structure, morphology, and the function of intrinsic renal cells, and promote disease progression [26]. Activation of ferroptosis is accompanied by excessive generation of ROS, leading to oxidative stress. The kidney and its cells contain abundant mitochondrial structures and are therefore highly vulnerable to oxidative stress. Therefore, persistent hyperglycemia in DN induces ferroptosis, leading to increased ROS levels in renal tissues and cells, which subsequently triggers intracellular oxidative stress and a cascade of pathological injuries [26,27]. Our findings further support this notion, demonstrating that AS-IV effectively reduces aberrantly activated ferroptosis in the kidneys of DN rats, thereby alleviating renal injury.

TFRC is a protein molecule with iron transport and endocytosis in cells [28], and there are two expression isoforms of TFR1 and TFR2 (hepatocyte-specific expression) in cells. Overexpression of TFRC may increase intracellular iron uptake and lead to excessive accumulation of iron ions, which may increase the risk of oxidative stress and ferroptosis [29]. In recent years, the role of TFRC in tumor cells has attracted considerable attention. The expression level of TFRC has been reported to be significantly upregulated in various malignancies, such as ovarian, colorectal

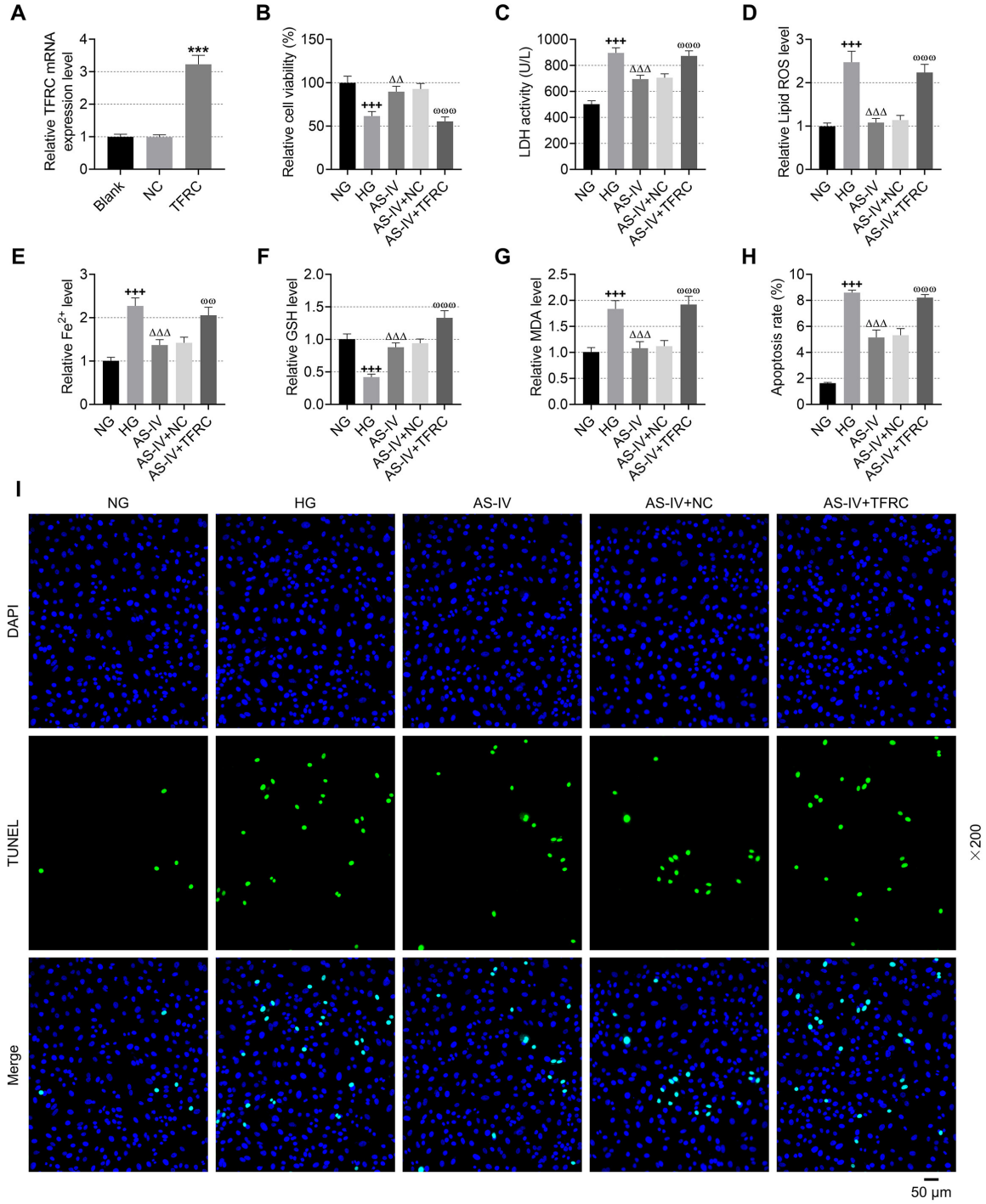

Fig. 5. TFRC overexpression partially reversed the effect of AS-IV on the HG-induced ferroptosis in HK-2 cells. (A) The transfection efficiency of TFRC was detected using qRT-PCR. (B) The effects of AS-IV and overexpressed TFRC on HG-induced cell viability were detected by Cell Counting Kit-8 assay. (C–G) Effects of AS-IV and overexpressed TFRC on HG-induced cellular ferroptosis were detected by the relevant kits. (H,I) The effects of AS-IV and overexpressed TFRC on HG-induced apoptosis were observed by TUNEL staining. The magnification was 200×. Scale bar = 50 μm. Data are presented as mean ± SD from three independent experiments, each performed in triplicate. ***$p < 0.001$ vs. NC group; +++$p < 0.001$ vs. NG; ΔΔ$p < 0.01$, ΔΔΔ$p < 0.001$ vs. HG; ωω$p < 0.01$, ωωω$p < 0.001$ vs. AS-IV+NC. Abbreviations: AS-IV, Astragaloside IV; NC, negative control; NG, normal group; HG, high glucose treatment; TFRC, transferrin receptor 1; LDH, lactate dehydrogenase; ROS, reactive oxygen species; MDA, malondialdehyde; GSH, glutathione.

and bladder cancers [30,31,32], and its overexpression is closely related to increased iron uptake, tumor cell proliferation and metastasis. In contrast, relatively few reports have investigated the role of TFRC in renal diseases. Previous

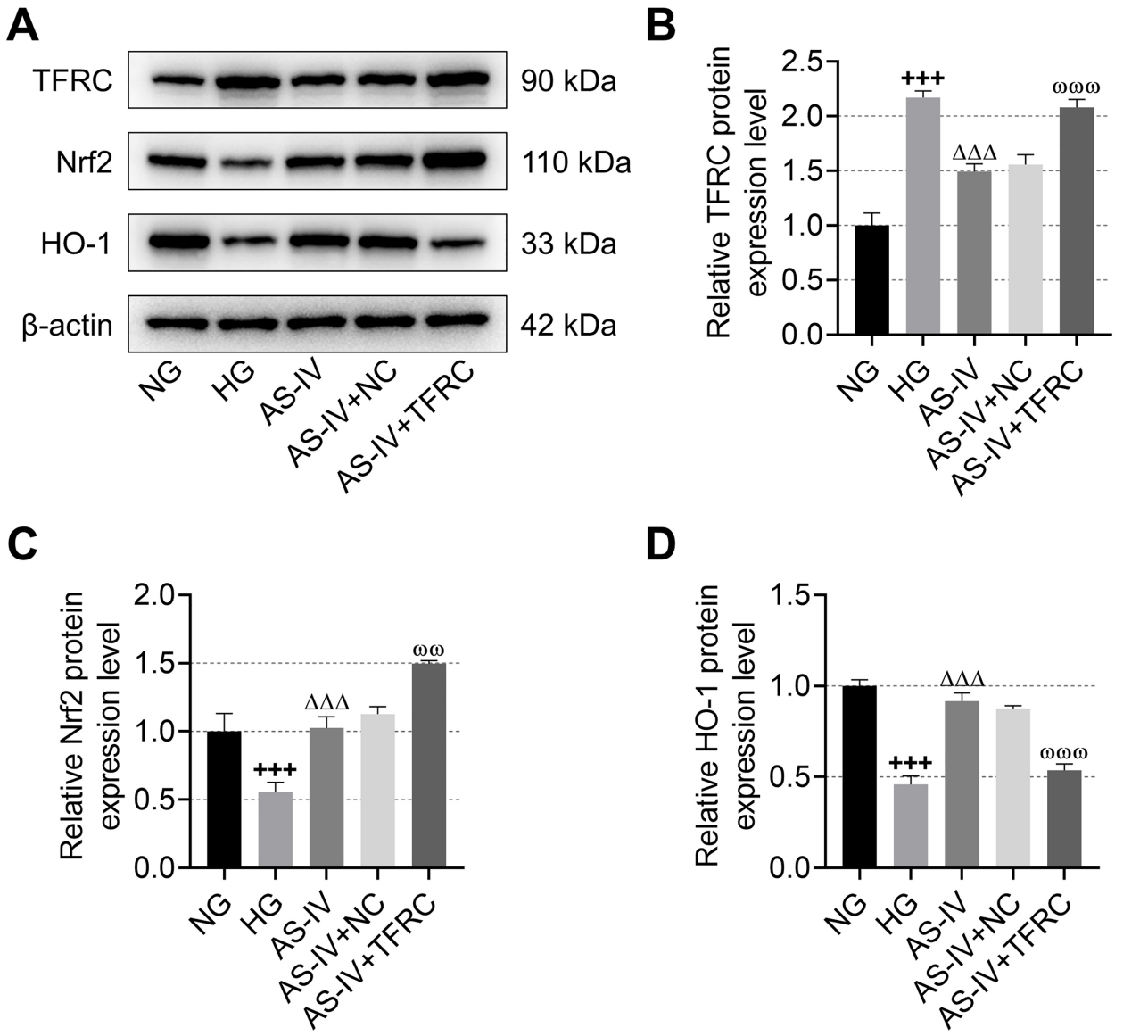

Fig. 6. TFRC overexpression partially reversed the effect of AS-IV on the Nrf2/HO-1 axis in HG-induced HK-2 cells. (A–D) Effects of AS-IV and overexpressed TFRC on TFRC/Nrf2/HO-1 protein expression in HG-induced cells were analysed by Western blotting. β-actin was the internal reference protein. Data are presented as mean ± SD from three independent experiments, each performed in triplicate. +++$p < 0.001$ vs. NG; ΔΔΔ$p < 0.001$ vs. HG; ωω$p < 0.01$, ωωω$p < 0.001$ vs. AS-IV+NC. Abbreviations: AS-IV, Astragaloside IV; NC, negative control; NG, normal group; HG, high glucose treatment; TFRC, transferrin receptor 1.

research has shown that knockdown of TFRC could alleviate renal fibrosis in DN mice [33]. In the present study, we further provided evidence that the effect of AS-IV on inhibition of excessive ferroptosis in cells may involve the targeted down-regulation of TFRC protein.

It is well established that Nrf2 is a key transcription factor that regulates cellular oxidative stress, coordinates cellular responses to oxidative stress, and induces the expression of various antioxidant genes, including HO-1. Activation of the Nrf2/HO-1 signalling pathway plays an important role in delaying the progression of DN, which reduces the accumulation of ROS and attenuates inflammatory responses [34,35]. Furthermore, Nrf2/HO-1 signalling also regulates ferroptosis during the course of DN. In the present study, we observed that AS-IV-mediated down-regulation of TFRC was associated with alterations in the ferroptosis process, an its effect correlated with activation of Nrf2/HO-1 signalling. Consistent with the present study, Wang et al. [36] demonstrated that activation of vitamin D receptor (VDR) inhibited ferroptosis in renal tubular epithelial cells through activation of Nrf2/HO-1 signalling. Similarly, the molecular mechanism by which quercetin alleviates ferroptosis hyperactivity is also through up-regulation of Nrf2/HO-1 [37].

In recent years, with rapid economic growth and lifestyle changes, the incidence of diabetes and its complication rates have been on the rise. According to statistics from the International Diabetes Federation (IDF) in 2019, the global number of people with diabetes was projected to reach 578.4 million by 2030 [38]. As the country with the largest diabetes population, China faces a rapidly increasing potential risk of DN. Therefore, the development of novel therapeutic agents is imminent. While our findings strongly support the therapeutic potential of AS-IV for DN, we acknowledge that a substantial gap remains between basic research and clinical application. Several important limitations of this study should be acknowledged regarding the mechanistic interpretation. First, the HG-induced HK-2 cell model did not include osmotic pressure controls such as mannitol or L-glucose, so we cannot exclude the possibility that hypertonic factors on cell damage and iron death indicators. Second, the STZ-induced diabetic model was established exclusively in male rats, which may not fully recapitulate the metabolic complexity of human diabetic nephropathy—particularly type 2 diabetes—and does not account for sex-related heterogeneity in disease progression or drug responses. Third, although TFRC was identified as a potential target of AS-IV through network pharmacology, the direct molecular interaction between AS-IV and TFRC remains to be validated. Fourth, this study lacks TFRC knockdown experiments and Nrf2 functional blockade experiments, which are necessary to establish the necessity and sufficiency of TFRC/Nrf2/HO-1 pathway in mediating the protective effects of AS-IV. Therefore, our current data do not support a complete linear signaling pathway model. Fifth, given that TFRC overexpression only partially reversed the protective effects of AS-IV *in vitro*, it is likely that AS-IV may exert its renoprotective effects through multiple targets and mechanisms beyond TFRC-dependent pathways, rather than a single TFRC-mediated mechanism. Sixth, our ferroptosis-related conclusions are based primarily on changes in marker expression and lipid peroxidation products—which are well-established phenotypic indicators—but several of these biochemical parameters were measured in serum rather than directly in renal tissue, thereby limiting the tissue-specific interpretation of our findings. Despite these limitations, our study provides supportive evidence linking AS-IV to the TFRC/Nrf2/HO-1/ferroptosis regulatory network in DN.

Conclusion

In summary, this study demonstrates that AS-IV attenuates renal injury and ferroptosis in DN, and these effects are associated with downregulation of TFRC and activation of the Nrf2/HO-1 antioxidant pathway. These findings suggest that TFRC may represent a promising therapeutic target and highlight the potential of AS-IV as a therapeutic candidate for DN.

Availability of Data and Materials

The datasets used or analyzed during the current study are available from the corresponding author upon reasonable request.

Author Contributions

FZ designed the research study; FZ and JLZ performed the research; JLZ collected and analyzed the data. FZ and JLZ have been involved in drafting the manuscript and both authors have been involved in revising it critically for important intellectual content. Both authors gave final approval of the version to be published. Both authors have participated sufficiently in the work to take public responsibility for appropriate portions of the content and agreed to be accountable for all aspects of the work in ensuring that questions related to its accuracy or integrity.

Ethics Approval and Consent to Participate

All animal experiments were approved by the Institutional Animal Care and Use Committee of Zhejiang Center of Laboratory Animals (Approval Number: ZJCLA-IACUC-20030149), and the experimental procedures followed the relevant regulations for the ethical protection of animals and the ARRIVE Guidelines 2.0.

Acknowledgment

Not applicable.

Funding

This work was supported by the Zhejiang Province Traditional Chinese Medicine Science and Technology Program [grant number: 2023ZR125].

Conflict of Interest

The authors declare no conflict of interest.

References

[1] Gupta S, Dominguez M, Golestaneh L. Diabetic Kidney Disease: An Update. The Medical Clinics of North America. 2023; 107: 689–705. https://doi.org/10.1016/j.mcna.2023.03.004

[2] Hu H, Zhang L, Li K. The Protective Effects and Mechanism of Mulberry Leaf Flavonoids on Type 2 Diabetic Nephropathy Mice. Journal of Experimental and Clinical Application of Chinese Medicine. 2024; 5: 56–58.

[3] Hu Q, Chen Y, Deng X, Li Y, Ma X, Zeng J, et al. Diabetic nephropathy: Focusing on pathological signals, clinical treatment, and dietary regulation. Biomedicine & Pharmacotherapy = Biomedecine & Pharmacotherapie. 2023; 159: 114252. https://doi.org/10.1016/j.biopha.2023.114252

[4] Wal P, Tyagi S, Pal RS, Yadav A, Jaiswal R. A Strategic Investigation on Diabetic Nephropathy; Its Conceptual Model and clinical Manifestations: A Review. Current Diabetes

Reviews. 2023; 19: e260422204036. https://doi.org/10.2174/1573399818666220426091238

[5] Martinez Leon V, Hilburg R, Susztak K. Mechanisms of diabetic kidney disease and established and emerging treatments. Nature Reviews. Endocrinology. 2026; 22: 21–35. https://doi.org/10.1038/s41574-025-01171-3

[6] Navaneethan SD, Zoungas S, Caramori ML, Chan JCN, Heerspink HJL, Hurst C, et al. Diabetes Management in Chronic Kidney Disease: Synopsis of the KDIGO 2022 Clinical Practice Guideline Update. Annals of Internal Medicine. 2023; 176: 381–387. https://doi.org/10.7326/M22-2904

[7] Gao X, Chen L, Zhang C, Gao H, Yang S, Huang G, et al. Treats the DKD in Mice by Regulating the TXNIP/NLRP3 Signaling Pathway. Clinical Traditional Medicine and Pharmacology. 2025; 6: 200245.

[8] Liu XJ, Hu XK, Yang H, Gui LM, Cai ZX, Qi MS, et al. A Review of Traditional Chinese Medicine on Treatment of Diabetic Nephropathy and the Involved Mechanisms. The American Journal of Chinese Medicine. 2022; 50: 1739–1779. https://doi.org/10.1142/S0192415X22500744

[9] Shen S, Zhong H, Zhou X, Li G, Zhang C, Zhu Y, et al. Advances in Traditional Chinese Medicine research in diabetic kidney disease treatment. Pharmaceutical Biology. 2024; 62: 222–232. https://doi.org/10.1080/13880209.2024.2314705

[10] Xue HZ, Chen Y, Wang SD, Yang YM, Cai LQ, Zhao JX, et al. Radix Astragali and Its Representative Extracts for Diabetic Nephropathy: Efficacy and Molecular Mechanism. Journal of Diabetes Research. 2024; 2024: 5216113. https://doi.org/10.1155/2024/5216113

[11] Liang Y, Chen B, Liang D, Quan X, Gu R, Meng Z, et al. Pharmacological Effects of Astragaloside IV: A Review. Molecules (Basel, Switzerland). 2023; 28: 6118. https://doi.org/10.3390/molecules28166118

[12] Wang Y, Zhang Z, Cheng Z, Xie W, Qin H, Sheng J. Astragaloside in cancer chemoprevention and therapy. Chinese Medical Journal. 2023; 136: 1144–1154. https://doi.org/10.1097/CM9.0000000000002661

[13] Yao M, Zhang L, Wang L. Astragaloside IV: A promising natural neuroprotective agent for neurological disorders. Biomedicine & Pharmacotherapy = Biomedecine & Pharmacotherapie. 2023; 159: 114229. https://doi.org/10.1016/j.biopha.2023.114229

[14] Tang JL, Xin M, Zhang LC. Protective effect of Astragalus membranaceus and Astragaloside IV in sepsis-induced acute kidney injury. Aging. 2022; 14: 5855–5877. https://doi.org/10.18632/aging.204189

[15] Li L, Dai Y, Ke D, Liu J, Chen P, Wei D, et al. Ferroptosis: new insight into the mechanisms of diabetic nephropathy and retinopathy. Frontiers in Endocrinology. 2023; 14: 1215292. https://doi.org/10.3389/fendo.2023.1215292

[16] Su L, Zhang J, Gomez H, Kellum JA, Peng Z. Mitochondria ROS and mitophagy in acute kidney injury. Autophagy. 2023; 19: 401–414. https://doi.org/10.1080/15548627.2022.2084862

[17] Sun X, Huang N, Li P, Dong X, Yang J, Zhang X, et al. TRIM21 ubiquitylates GPX4 and promotes ferroptosis to aggravate ischemia/reperfusion-induced acute kidney injury. Life Sciences. 2023; 321: 121608. https://doi.org/10.1016/j.lfs.2023.121608

[18] Li J, Zhang H. Protective Effects of Propofol on Acute Kidney Injury Through Suppressing Ferroptosis and Inflammatory Responses in Renal Tubular Epithelial Cells. Discovery Medicine. 2025; 37: 3095–3106. https://doi.org/10.24976/Discov.Med.202537203.259

[19] Stockwell BR, Friedmann Angeli JP, Bayir H, Bush AI, Conrad M, Dixon SJ, et al. Ferroptosis: A Regulated Cell Death Nexus Linking Metabolism, Redox Biology, and Disease. Cell. 2017; 171: 273–285. https://doi.org/10.1016/j.cell.2017.09.021

[20] Gaschler MM, Stockwell BR. Lipid peroxidation in cell death. Biochemical and Biophysical Research Communications. 2017; 482: 419–425. https://doi.org/10.1016/j.bbrc.2016.10.086

[21] Tang L, Zhou F, Wang Y, Jiao Y. The E3 Ubiquitin Ligase MIB2 Exacerbates Sepsis-Associated Acute Kidney Injury by Promoting GPX4 Degradation-Mediated Ferroptosis and Mitochondrial Dysfunction. Discovery Medicine. 2025; 37: 2041–2054. https://doi.org/10.24976/Discov.Med.202537200.175

[22] Lei X, Zhang L, Li Z, Ren J. Astragaloside IV/lncRNA-TUG1/TRAF5 signaling pathway participates in podocyte apoptosis of diabetic nephropathy rats. Drug Design, Development and Therapy. 2018; 12: 2785–2793. https://doi.org/10.2147/DDDT.S166525

[23] Kim S, Kang SW, Joo J, Han SH, Shin H, Nam BY, et al. Characterization of ferroptosis in kidney tubular cell death under diabetic conditions. Cell Death & Disease. 2021; 12: 160. https://doi.org/10.1038/s41419-021-03452-x

[24] Otsuki M, Fukuda N, Inoue T, Mineshige T, Otsuki T, Horikoshi S, et al. Preclinical Study of DNA-Recognized Peptide Compound Pyrrole-Imidazole Polyamide Targeting Human TGF-β1 Promoter for Progressive Renal Diseases in the Common Marmoset. Molecules (Basel, Switzerland). 2019; 24: 3178. https://doi.org/10.3390/molecules24173178

[25] Ji J, Tao P, Wang Q, Cui M, Cao M, Xu Y. Emodin attenuates diabetic kidney disease by inhibiting ferroptosis via upregulating Nrf2 expression. Aging. 2023; 15: 7673–7688. https://doi.org/10.18632/aging.204933

[26] Chen Y, Huang G, Qin T, Zhang Z, Wang H, Xu Y, et al. Ferroptosis: A new view on the prevention and treatment of diabetic kidney disease with traditional Chinese medicine. Biomedicine & Pharmacotherapy = Biomedecine & Pharmacotherapie. 2024; 170: 115952. https://doi.org/10.1016/j.biopha.2023.115952

[27] Hong J, Li X, Hao Y, Xu H, Yu L, Meng Z, et al. The PRMT6/STAT1/ACSL1 axis promotes ferroptosis in diabetic nephropathy. Cell Death and Differentiation. 2024; 31: 1561–1575. https://doi.org/10.1038/s41418-024-01357-8

[28] Yi L, Hu Y, Wu Z, Li Y, Kong M, Kang Z, et al. TFRC upregulation promotes ferroptosis in CVB3 infection via nucleus recruitment of Sp1. Cell Death & Disease. 2022; 13: 592. https://doi.org/10.1038/s41419-022-05027-w

[29] Feng H, Schorpp K, Jin J, Yozwiak CE, Hoffstrom BG, Decker AM, et al. Transferrin Receptor Is a Specific Ferroptosis Marker. Cell Reports. 2020; 30: 3411–3423.e7. https://doi.org/10.1016/j.celrep.2020.02.049

[30] Huang Y, Huang J, Huang Y, Gan L, Long L, Pu A, et al. TFRC promotes epithelial ovarian cancer cell proliferation and metastasis via up-regulation of AXIN2 expression. American Journal of Cancer Research. 2020; 10: 131–147.

[31] Kim H, Villareal LB, Liu Z, Haneef M, Falcon DM, Martin DR, et al. Transferrin Receptor-Mediated Iron Uptake Promotes Colon Tumorigenesis. Advanced Science (Weinheim, Baden-Wurttemberg, Germany). 2023; 10: e2207693. https://doi.org/10.1002/advs.202207693

[32] Qin J, Li Z, Su L, Wen X, Tang X, Huang M, et al. Expression of transferrin receptor/TFRC protein in bladder cancer cell T24 and its role in inducing iron death in bladder cancer. International Journal of Biological Macromolecules. 2024; 274: 133323. https://doi.org/10.1016/j.ijbiomac.2024.133323

[33] Yasumura S, Naito Y, Okuno K, Sawada H, Asakura M, Masuyama T, et al. Effects of Heterozygous TfR1 (Transferrin Receptor 1) Deletion in Pathogenesis of Renal Fibrosis in Mice. Hypertension (Dallas, Tex. : 1979). 2020; 75: 413–421. https://doi.org/10.1161/HYPERTENSIONAHA.119.13670

[34] Lv C, Cheng T, Zhang B, Sun K, Lu K. Triptolide protects against podocyte injury in diabetic nephropathy by activating the Nrf2/HO-1 pathway and inhibiting the NLRP3 inflammasome pathway. Renal Failure. 2023; 45: 2165103. https://doi.org/10.1080/0886022X.2023.2165103

[35] Hasan IH, Shaheen SY, Alhusaini AM, Mahmoud AM. Simvastatin mitigates diabetic nephropathy by upregulating farnesoid X receptor and Nrf2/HO-1 signaling and attenuating oxidative stress and inflammation in rats. Life Sciences. 2024; 340: 122445. https://doi.org/10.1016/j.lfs.2024.122445

[36] Wang H, Yu X, Liu D, Qiao Y, Huo J, Pan S, et al. VDR Activation Attenuates Renal Tubular Epithelial Cell Ferroptosis by Regulating Nrf2/HO-1 Signaling Pathway in Diabetic Nephropathy. Advanced Science (Weinheim, Baden-Wurttemberg, Germany). 2024; 11: e2305563. https://doi.org/10.1002/advs.202305563

[37] Feng Q, Yang Y, Qiao Y, Zheng Y, Yu X, Liu F, et al. Quercetin Ameliorates Diabetic Kidney Injury by Inhibiting Ferroptosis via Activating Nrf2/HO-1 Signaling Pathway. The American Journal of Chinese Medicine. 2023; 51: 997–1018. https://doi.org/10.1142/S0192415X23500465

[38] Saeedi P, Petersohn I, Salpea P, Malanda B, Karuranga S, Unwin N, et al. Global and regional diabetes prevalence estimates for 2019 and projections for 2030 and 2045: Results from the International Diabetes Federation Diabetes Atlas, 9th edition. Diabetes Research and Clinical Practice. 2019; 157: 107843. https://doi.org/10.1016/j.diabres.2019.107843